



Research

Cite this article: Knapp A, West T, Early CM, Felice RN. 2025 Avian cranial evolution is influenced by shape interactions between hard and soft tissue traits. *Proc. R. Soc. B* **292**: 20250848.
<https://doi.org/10.1098/rspb.2025.0848>

Received: 28 March 2025

Accepted: 14 November 2025

Subject Category:

Evolution

Subject Area:

evolution

Keywords:

geometric morphometrics, birds, phenotypic evolution, adaptive evolution, evolutionary trade-offs

Author for correspondence:

Andrew Knapp
e-mail: ucfaakn@ucl.ac.uk

Electronic supplementary material is available online at <https://doi.org/10.6084/m9.figshare.c.8168691>.

Avian cranial evolution is influenced by shape interactions between hard and soft tissue traits

Andrew Knapp^{1,2}, Taylor West³, Catherine M. Early⁴ and Ryan N. Felice^{1,2}

¹Department of Cell and Developmental Biology, University College London, London WC1E 6BT, UK

²Department of Science, Natural History Museum, London SW7 5BD, UK

³University College London, London, UK

⁴Biology Department, Science Museum of Minnesota, Saint Paul, MN 55102, USA

ID AK, 0000-0003-4822-5623; TW, 0000-0001-8933-3773; CME, 0000-0003-0308-2710

Changes in the structure and relative size of the brain are thought to be key transformations in the evolution of birds, reflecting innovations and diversity of neurosensory and cognitive capabilities. These changes do not occur in isolation, being accompanied by many other derived morphological characteristics. In the avian head alone, these include the evolution of a toothless beak, an increase in relative eye size, and a reduction and restructuring of jaw muscles. Several developmental trade-offs have been proposed to explain the interrelationships among these traits, but how these developmental patterns translate into evolutionary correlations among cranial traits is poorly understood. Here, we use two-block partial least squares analyses and Ornstein–Uhlenbeck models of adaptive trait evolution to explore the phenotypic evolution of hard and soft cranial tissues and test hypotheses of correlated trait evolution. In pairwise analyses, we found that all traits are significantly correlated, and found support for a form of adaptive trait evolution across the whole head in which traits interact reciprocally via the neurocranium. Together, these results highlight the integrated nature of the avian head and reveal that the evolution of diverse phenotypes is a result of complex multiple interactions among hard and soft tissue traits.

1. Introduction

Among the many phenotypic changes associated with the origin of modern birds, one of the most striking is the increase in brain volume relative to body size compared with non-avian theropod dinosaurs. This increase in relative brain size is also associated with differential expansion and restructuring of regions of the brain associated with cognition and vision [1–7]. In modern birds, variation in brain structure and function underlie a broad range of complex behaviours, including sociality, vocal learning, parental care and flight [2,8–12]. Indeed, many researchers have proposed that the evolution of brain shape and size is a key factor influencing the ecological diversification of the clade [13–15]. As such, understanding the factors that influence neuroanatomical evolution across the avian tree of life has been a key area of research focus [13,16,17].

There is strong comparative and experimental evidence that the shape and relative proportions of functional regions of the brain reflect their processing capacities because of the corresponding increase in the number of neurons [7,18]. Sometimes called the ‘principle of proper mass’, this structure-to-function mapping is typically thought of as the primary driver of neuroanatomical evolution and allows for cognitive, sensory and behavioural traits to be reconstructed in extinct taxa [1,2,5,13,17,19–23]. For example, long-distance

migratory birds have enlarged optic lobes, presumably as a result of selection on high visual acuity [15]. Similarly, the high cognitive ability in famously intelligent birds such as parrots and crows is reflected in the presence of a relatively larger cerebrum (forebrain) [9,12,14,24].

To date, most research into the evolution of brain shape variation across birds has focused on the influence of the function of the brain itself [7,9,12–14,25] or of allometry [2,4–6,17,26]. However, the ontogenetic growth of the brain is strongly correlated with many other cranial structures, and these correlations might impose constraints that also contribute to patterns of brain shape evolution [27]. For example, eye and brain shape are significantly correlated in birds, and differences in brain shape are further associated with the orientation of the neck and thus head posture [26]. Increased encephalization may also impact the evolution of other soft tissues. The rostrocaudal orientation of jaw muscles in neognath birds differs markedly from the more vertically orientated jaw muscles in their extinct theropod relatives, and it has been proposed that these radical changes have been caused by the lateral expansion of the brain in modern birds [28]. This ultimately led to the evolution of powered cranial kinesis in neognaths, in part to compensate for the resultant reduction in mechanical efficiency of the restructured jaw musculature [28].

The shape of the brain and neurocranium are tightly linked during development [29–35] because the brain originates early in embryological development and influences the formation of the surrounding protective skull tissue [34,36,37]. As a result, changes in brain and skull shape track each other closely through both development and evolution [38,39]. This observation gives support to the ‘Hand in Glove’ hypothesis, which proposes that the brain is the primary influence on neurocranium morphology and, in turn, provides structure and support for the surrounding soft tissues, including the jaw muscles and eyes [26,40,41]. Conversely, the development of the skull may itself affect brain shape and size. Research into craniosynostosis (premature fusion of cranial sutures) in humans has revealed that resultant changes in relative growth of the overlying skull bones can impact the shape of the enclosed brain [41,42]. This implies that postnatal skeletal growth may influence the subsequent development of the brain, despite the morphogenetic primacy of the brain in early embryogenesis.

The ‘Spatial Packing Hypothesis’ (SPH) predicts that the head has a finite capacity to accommodate and maintain the functional integrity of a range of structures, and that the size, shape and position of anatomical structures impact, and are impacted by, the growth and development of the surrounding tissues [43]. One example of spatial packing trade-offs in vertebrates comes from experiments on mice with myostatin deficiency, which results in increased muscle volume, including the jaw muscles attached to the temporal region of the skull. These mutant lines developed a smaller brain volume than wild-type mice, suggesting that jaw muscles and the brain compete for space in the head [43,44]. Under normal muscle growth, however, trade-offs may not operate in the same way. Jaw muscle growth in domestic chickens (*Gallus gallus*) exhibits positive allometry relative to eye and brain volume, indicating that space within the head is not a limiting factor for soft tissue growth in this species [45]. In another example from birds, the brain and eyes both occupy a large volume of the head and therefore compete for space within it, with the size of the head itself defining the upper volume limit of these components [46]. One notable result of this is that an increase in relative brain size combined with a shortened basicranial length may lead to increased basicranial flexion, driven by the restructuring of cranial traits to accommodate this increase [47–49]. Either a trade-off in volume or a change in the shape of these structures to accommodate them both within the head may therefore be expected when any major changes in size or shape occur, but the extent to which these patterns extend to shape, rather than size, and across taxa has not been explored.

Finally, the ‘Functional Matrix Hypothesis’ states that the form of the skull, along with its growth and maintenance, are related to the functional demands of the soft tissues that are associated with the skull [50,51]. Skull growth is mediated by the mechanical forces imposed by the non-skeletal tissues of the head, such as the growing brain and cranial muscles [52], and the head develops as part of a functional complex of hard and soft tissues that is shaped by mechanical and functional demands. This hypothesis has received support from embryological experiments in mice that showed neuronal function and peripheral innervation were crucial for normal craniofacial development [53].

Together, these interrelated hypotheses leverage evidence from embryology to explain the correlated development of the skull, brain, eye and cranial muscle tissues. The consequences of these developmental interactions between cranial tissues are poorly understood across macroevolutionary time scales, however, and the effects of selection on different structures of the skull cannot be fully understood without first unravelling these interactions [54]. Moreover, it remains unknown how the phenotypic evolution of the brain is influenced by interactions with the other well-studied structures of the avian head, such as the beak [55–57], because although its shape is often analysed in relation to the neurocranium, its relationship to brain shape is rarely considered [58–62]. Here, we use evolutionary modelling to explore three-dimensional (3D) shape variation among the skull, brain, orbit and jaw musculature across a sample of 322 extant and recently extinct avian taxa to determine how interactions among cranial traits mediate phenotypic evolution under natural selection in birds. Integrating three-dimensional shape analysis with these methods improves upon linear and volumetric analyses by incorporating more information not only about how structures vary between species but also how their phenotypic variation impacts that of other associated traits, allowing us to describe the effects of correlated trait evolution. We first investigate pairwise evolutionary correlations between hard and soft tissue structures using a two-block partial least squares (PLS) approach. We then compare several competing evolutionary hypotheses by integrating these traits across the head for the first time using Ornstein–Uhlenbeck (OU) models of adaptive trait evolution, implemented with *mvSLOUCH* [63,64]. We predict that phenotypic integration is significant across all the major hard and soft tissue components of the avian head and that the brain plays a key role in influencing its phenotypic evolution, but that its influence is moderated by evolutionary interactions between the surrounding hard and soft tissues.

2. Material and Methods

(a) Mesh generation

We assembled a dataset of computed tomography (CT) scans of the skulls of 322 birds (311 extant, 11 extinct; see electronic supplementary material for specimen sources). Taxa were chosen to represent the taxonomic and morphological diversity of modern birds, incorporating 43 of 44 Orders (excluding Tinamiformes), 188 of 254 Families and 322 of 2392 Genera (electronic supplementary material, figure S1) [65]. We created three-dimensional skull meshes segmented from μ CT data [66,67] and decimated them to 1 million faces. We used the ‘endomaker’ function in the R package *Arothron* [68] to create endocasts of all specimens. We manually removed the remnants of cranial nerve V from the endocast, which superficially overlays the optic lobe, to allow for consistent surface semilandmark placement on this structure.

(b) Phylogeny

We generated an informal supertree containing all 11 extinct and 311 extant taxa in our sample. Recent phylogenetic analyses using genomic data have generated new hypotheses regarding the broad-scale (i.e. family level and higher) relationships among Neoaves (electronic supplementary material, figure S1) [69]. We thus used this recent topology as a backbone tree upon which to graft subfamily-level relationships derived from a comprehensive clade-wide phylogeny [70]. We downloaded 1000 trees from the posterior distribution of species-level Neoaves phylogenies from BirdTree.org using the ‘Hackett Stage 2’ topologies [70]. Using Tree Annotator, we generated a single maximum clade credibility (MCC) tree from this posterior sample under the ‘target heights method’ [71]. We extracted individual clades from this MCC and grafted them to the corresponding positions in the backbone tree using established approaches [72]. The resulting supertree contains 9993 extant taxa with the broad-scale phylogenetic relationships and divergence times supported by the recent genomic analysis.

Finally, we added extinct taxa that are not present in the BirdTree.org [70] topology using two approaches. For very recently extinct taxa with well-resolved phylogenetic affinities (e.g. *Ninox albifacies*, *Moho braccatus*), we simply substituted them with their most closely related extant taxa (*Ninox rufa*, *Hypocolius ampelinus*, respectively) [73]. For other extinct taxa (i.e. *Aptornis otidiformis*, *Cnemiornis calcitrans*, *Diaphorapteryx hawkinsi*, *Emeus crassus*, *Eudyptes warhami*, *Pezophaps solitaria* and *Raphus cucullatus*) we used the ‘tree.merger’ function of the *RRphylo* R package [74] to attach extinct taxa to known positions on the topology [75–80].

(c) Geometric morphometrics

We applied landmarks to the right hemisphere of both the skull and endocast using templates adapted from Mitchell *et al.* [81] and Watanabe *et al.* [17], respectively, using Stratovan Checkpoint v.2020.10.13.0859 [82] (electronic supplementary material, figures S2 and S3). Discrete anatomical (Bookstein Type I and II) landmarks were used to describe homologous points, and semilandmark curves were used to capture homologous curves and sutures (electronic supplementary material). The skull landmark template was modified to more comprehensively quantify jaw muscle shape (MS; adductor mandibulae externus and depressor mandibulae) [83] by placing semilandmark curves on the skull along the margins of the fossa musculorum temporalium and impressio musculi depressor mandibulae as proxies for MS (electronic supplementary material, figure S2) [84]. To optimize coverage and prevent oversampling of landmark data, we assessed semilandmark density with the ‘LaSEC’ function in the R package *LaMBDA* [85]. This resulted in a total of 20 anatomical and 190 semilandmarks in 21 curves for the skull, and 14 anatomical and 72 semilandmarks in 15 curves for the endocast (electronic supplementary material). The homologous structures of the endocast (cerebrum, optic lobe, cerebellum and medulla) have well-defined borders [17], but the globular, smooth surfaces have no reliably identifiable points for placing landmarks. Large areas of the endocast surface, therefore, cannot be captured using anatomical landmarks or semilandmark curves. Following Watanabe *et al.* [17], we used a semi-automated method to place surface semilandmarks on the surface of these structures in addition to the manually placed anatomical landmarks and semilandmark curves. We used a single specimen (*Anhinga anhinga*) to create a template of 103 surface semilandmarks and then used a semi-automated procedure in the R package *Morpho* [86] to apply the patch to all endocast specimens [87]. This approach uses our manually placed anatomical landmarks and semilandmark curves to delimit anatomical regions of the endocast for automated surface semilandmark placement and retains them in further analyses. The resulting patched specimens were manually inspected to ensure consistent surface semilandmark placement, following Bardua *et al.* [87]. We measured the maximum linear distance of the orbit on the neurocranium as a proxy for eye size (ES). To account for absolute size differences between taxa, we standardized orbit diameter with the centroid size of the neurocranium, which was obtained by the Procrustes fit of neurocranium landmarks [88]. Previous studies have shown a nonlinear relationship between brain volume and body mass in birds [6,16,26], so we used neurocranium size to scale orbit diameter because these traits scale more linearly than with body mass.

We slid semilandmarks to minimize bending energy and then reflected landmarks across the midline for both skull and endocast to ensure bilateral symmetry, a protocol that prevents lateral deviation from the midline that can be induced during landmark alignment [89]. Symmetrized landmark data were aligned with a general Procrustes alignment using the ‘procSym’ function in the R package *Morpho* [86]. We performed global alignment separately for the whole skull and endocast landmark set, and separate (local) alignments of the different regions of the skull (neurocranium, rostrum and jaw muscles) to minimize autocorrelation with other regions that may arise from the redistribution of variation that occurs in global alignments of

landmarks [89]. After alignment, we removed reflected landmarks and performed all subsequent analyses on the right-side landmarks for each landmark subset. We explored shape variation by performing a principal components analysis (PCA) on the Procrustes-aligned shape data for the whole skull and for each subset of landmarks (endocast, neurocranium, jaw muscles and rostrum), using the ‘gm.prcomp’ function in the R package *geomorph* [90].

The correlation of shape with size (allometry) may have significant effects on trait integration [54,91,92]. We accounted for these effects by performing a phylogenetic regression of Procrustes shape variables against log-transformed mean species body mass, using the ‘procD.pgls’ function in the R package *geomorph* [90]. We took mean body mass for each species from the AVONET trait database [93] for extant birds and used a combination of published values and scaling equations from Field *et al.* [94] to estimate body mass from hindlimb bone dimensions for extinct taxa (electronic supplementary material, table S1 for details). We created allometry-corrected PCAs to explore the effects of size-related variation using the residual shape components of these regressions [56].

(d) Pairwise correlation

To test evolutionary correlations between traits, we performed two-block PLS analyses for each pairwise trait combination (rostrum shape (RS), endocast shape, neurocranium shape, jaw MS and ES) using the ‘phylo.integration’ function in the R package *geomorph* [90,95–97] with Procrustes-aligned landmark data, and log-transformed values for ES. Sliding semilandmarks to minimize bending energy may occasionally overinflate integration values [98]. To ensure that this did not affect our results, we reran all two-block PLS analyses using a separate dataset created with the Procrustes distance method (PDM) for semilandmark sliding.

(e) Evolutionary modelling

We modelled the correlated evolution of cranial hard and soft tissues to test the hypothesis that selection for brain shape influences the evolution of the skull, eyes and jaw muscles, and *vice versa*. We used a multivariate OU model of adaptive evolution as implemented in the R package *mvSLOUCH* v.2.7.6 [63,64], an approach that uses established methods that can correct for measurement error and are robust to Type I error [99]. Under the multivariate OU model, traits are pulled towards an adaptive optimum or optima by an attractive force that is interpreted as natural selection, and the strength of this selection is described by the matrix A. The diagonal elements of the A matrix describe the selection on individual traits, and the off-diagonal elements represent the degree to which traits’ paths towards the optimum influence each other [63,64]. The strength of the *mvSLOUCH* approach to modelling multivariate OU processes is that specific hypotheses of trait interactions and correlations can be evaluated by specifying the properties of the A matrix. The tempo of adaptation, expressed as phylogenetic half-lives for each eigenvector of the A matrix in the best-supported model, is also provided by *mvSLOUCH*. Half-lives represent rates of adaptation of the set of traits towards the primary optimum along the directions in trait space described by that eigenvector, measured as the time needed for the effect of the initial state to be halved and are recommended as current best practices for appropriate interpretation of OU models [63,99]. It is important to note that, because this is a multivariate analysis, these half-lives refer to the adaptation of a group of complex traits rather than a single trait, as would be implied in a univariate model.

We formulated 12 hypotheses to investigate evolutionary correlations among our sampled traits (table 1), constructing an A matrix for each hypothesis to define trait interactions (electronic supplementary material, table S1) [64]. Our models were based on the three main hypotheses of correlated trait evolution (Hand in Glove, Spatial Packing and Functional Matrix). For each hypothesis, we designed a model of trait interactions which best fits the set of traits that we sampled and designed a second model that involves feedback between traits. We designed a third SPH in which jaw MS is not directly influenced by brain shape but instead evolves in response to rostrum (i.e. beak, palatal bones and jugal) shape. This is based on the observation that there is minimal trade-off between brain size and jaw muscle size during embryonic and early postnatal growth of *G. gallus* [45]. In addition, we included ‘Ecological Selection’ models, which imply that RS, which dominates morphological variation across birds [56,60], is a direct result of selection as opposed to the developmental by-product of shape changes in other traits. Finally, we created a ‘Modular’ model, in which the head is divided into two non-interacting phenotypic modules, the neurosensory module, composed of the endocast, neurocranium and relative orbit diameter, and the feeding module, composed of the rostrum and jaw muscles. These regions comprise the two major components of the kinetic avian skull [28] and are derived from separate developmental centres, namely the mandibular cranial neural crest (rostrum) and mesoderm (neurocranium) [31]. This model accounts for the possibility that developmental modularity leads to mosaic evolution in the avian head [59] and may be an important factor in the evolution of cranial kinesis in modern birds [28]. All hypotheses were contrasted with the Brownian motion null model of no selection on any trait. We conducted two sets of analyses for each model to explore differences in trait evolution that are not connected with adaptation, e.g. developmental correlations. In the first set, we assigned the stochastic perturbations matrix (Σ_{yy}) to be diagonal, implying no interactions between the traits in the non-adaptive component of evolution. In the second set, Σ_{yy} was upper-triangular, indicating interacting evolution of the traits due to non-adaptive effects. We repeated these analyses using PC scores from the allometry-corrected PCAs for each trait to account for allometric effects on shape. Using allometry-corrected shape data allows us to account for the effects of body size in our models without the significant increases in model complexity that adding an extra trait (i.e. body mass) and its associated interactions would incur. We compared Akaike information criterion (AICc) scores to determine the best-supported model,

determining confidence intervals for each model parameter by performing 100 parametric bootstraps on the highest likelihood model.

Previous research has suggested broader-scale phylogenetic patterns of relative brain size among extant birds [5,14,48]. Australaves is a monophyletic clade composed of Passeriformes, Psittaciformes, Falconiformes and Cariamiformes, and contains taxa with the largest relative brain sizes among extant birds [9,12]. Palaeognathae, by contrast, generally have low relative brain sizes compared with most birds [19] and do not possess the highly kinetic craniofacial and palatal region of neognaths [28]. We therefore subdivided our dataset into Australaves, Palaeognathae and ‘other’ to investigate how trait optima differ between these groups in the best-supported model.

3. Results

Variation in whole-skull shape in the dataset is dominated by variation in RS (electronic supplementary material, figure S4). The major axis of shape variation in whole-skull shape data (PC1) is elongation, representing 45% of total skull shape variation, and with short-skulled (brachycephalic) taxa at negative PC values and long-skulled (dolichocephalic) taxa at positive PC values. This is followed by variation in rostrum depth (PC2; 10.3% of total shape variation) and relative orientation of the rostrum and foramen magnum (PC3; 9.86% of total shape variation). Similar patterns are seen when the skull is broken down into component parts. The major axis of shape variation in the rostrum is elongation (PC1; 46.1% of total shape variation), as it is with neurocranium shape (PC1; 25.2% of total shape variation; electronic supplementary material, figure S6). Variation in jaw MS is largely driven by differences in the relative size of the adductor mandibulae and the depressor mandibulae attachment sites, with 48% of shape variation accounted for by relative expansion of the adductor mandibulae (electronic supplementary material, figure S7). The first two PC axes of the endocast make similar contributions to total shape variation (PC1 = 33.1%; PC2 = 25.6%) and correspond to relative expansion of the cerebrum and flexion of the basicranial angle, and elongation of the whole brain, respectively (electronic supplementary material, figure S8). Allometry is significant for all subsets of shape data but accounts for relatively little total shape variation (1.6% in rostrum to 9.3% in neurocranium; electronic supplementary material, table S2). Consequently, allometry-corrected PCAs are very similar to their raw shape data counterparts, except for neurocranium shape (electronic supplementary material, figure S9).

All trait pairs are significantly correlated ($p < 0.05$), indicating strong evolutionary integration in the head of crown birds (figure 1; electronic supplementary material, table S3). As with individual shape variation (electronic supplementary material, figures S4–S8), elongation is the dominant form of shape variation of individual traits in each pairwise analysis of trait correlation (electronic supplementary material, figure S10). This effect is most obvious with RS, which shows clear elongation in correlation with neurocranium elongation (electronic supplementary material, figure S9F and S9J), and with endocast elongation and ventral flexion (electronic supplementary material, figure S9E and S9A). Similarly, lengthening of the rostrum is correlated with enlargement and elongation of the attachment area of the adductor mandibulae (electronic supplementary material, figure S9G and S9N). The dominant form of neurocranium covariation with all other traits is also elongation. For example, more elongate neurocrania are associated with a relatively enlarged adductor mandibulae attachment site (electronic supplementary material, figure S9K and S9O). Basicranial flexion of the endocast is apparent to varying amounts in all two-block PLS analyses. This effect is most obvious with orbit diameter, where a higher flexion angle is associated with relatively larger orbits (electronic supplementary material, figure S9D). Flexion of the brain in these instances resembles the shape variation seen along PC1 of the PCA for brain shape, where more acute angles are associated with a larger cerebrum (electronic supplementary material, figure S8).

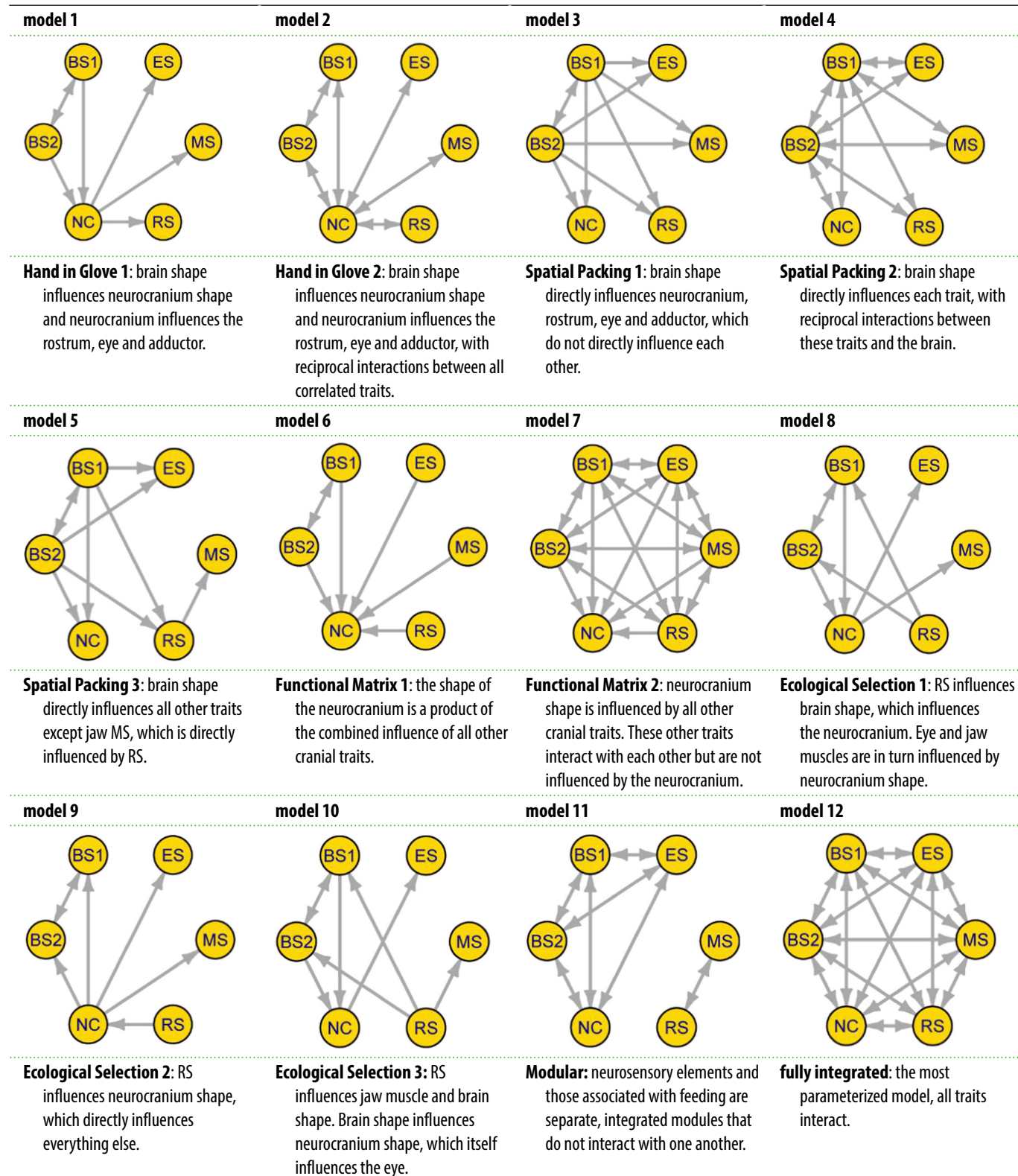
Reanalysing the landmark data after sliding the curve and surface semilandmarks using the PDM made no appreciable difference to either the significance or r-PLS results of any two-block PLS (electronic supplementary material, table S4), and shape transformations for all pairwise analyses remain the same. Similarly, all two-block PLS analyses are significant for allometry-corrected shape data and reveal no major differences in either r-PLS or effect size scores to the analyses with uncorrected shape data (electronic supplementary material, table S5).

The *mvSLOUCH* analysis recovered best support for the Hand in Glove 2 model of trait interactions with diagonal Σ_{yy} (AIC weight = 0.85; electronic supplementary material, table S6). Support for the diagonal Σ_{yy} indicates that there are no interactions between traits in the noise component of evolution in this model. Interactions in the A matrix (pull toward adaptive optima) occur directly between brain shape and neurocranium shape, as well as between neurocranium shape and RS, jaw MS and orbit diameter. Adaptive evolution of brain shape, therefore, only directly influences adaptive evolution of the surrounding neurocranium in this model. The next best-supported model is Modular, with an AIC weight of 0.15 ($\Delta\text{AIC}_c = 3.46$; electronic supplementary material, table S6). In this model, traits are separated into a neurosensory module and a feeding module, with adaptive interactions between traits within modules, but weak interactions between traits in different modules. The results of the *mvSLOUCH* analysis performed on the allometry-corrected shape data also show the strongest support for Hand in Glove 2 with diagonal Σ_{yy} and Modular as the next best-supported model ($\Delta\text{AIC}_c = 3.62$; electronic supplementary material, table S7).

Rates of adaptation, measured as phylogenetic half-lives, are relatively consistent across eigenvectors and range from 62.46% to 82.81% of tree height, translating to 55.3–73.3 Ma (table 2). Each eigenvector reveals the adaptive contribution of traits via loadings. For example, eigenvector 1 (e_1) is driven primarily by jaw MS (0.99), with minor contributions from other traits, notably neurocranium shape (NC; 0.10). Rates of adaptation for allometry-adjusted shape data show very similar patterns to raw shape data (electronic supplementary material, table S8), with jaw MS dominating e_1 , and rates of adaptation are comparable to those of raw shape data.

Trait optima values vary between subsets of taxa for all traits and are especially noticeable in brain shape (figure 2). Palaeognathae and Australaves have positive optima for the first axis of brain shape variation (BS1), indicating that these

Table 1. Correlated trait models tested with *mvSLOUCH*. Diagrams on the left represent model interactions. Circles represent traits, and arrows represent the direction of trait influence. Traits are NC = neurocranium shape; BS1 and BS2 = PCs 1 and 2 of endocast shape, respectively; ES = relative orbit diameter; MS = jaw muscle shape; RS = rostrum shape. See electronic supplementary material, table S3, for corresponding A matrices.



groups have tended to evolve a relatively larger cerebrum than taxa in the 'other' group, which have a negative shape optimum value. In contrast, Palaeognathae have a negative optimum value along the second axis of brain shape variation (BS2), corresponding to a more elongate endocast with a posteriorly oriented brain stem. Palaeognathae also differ noticeably from other groups by having an elongate neurocranium shape optimum (NC) and having a relatively larger orbit diameter (ES). All three groups have a similar optimum for RS and jaw MS. Some differences are apparent in trait optima for allometry-adjusted shape data (electronic supplementary material, figure S11), notably in brain and jaw MS. Palaeognathae brain shape optima are nearer the mean value for both axes of shape variation, whereas the jaw muscle optimum has a more positive value in this clade.

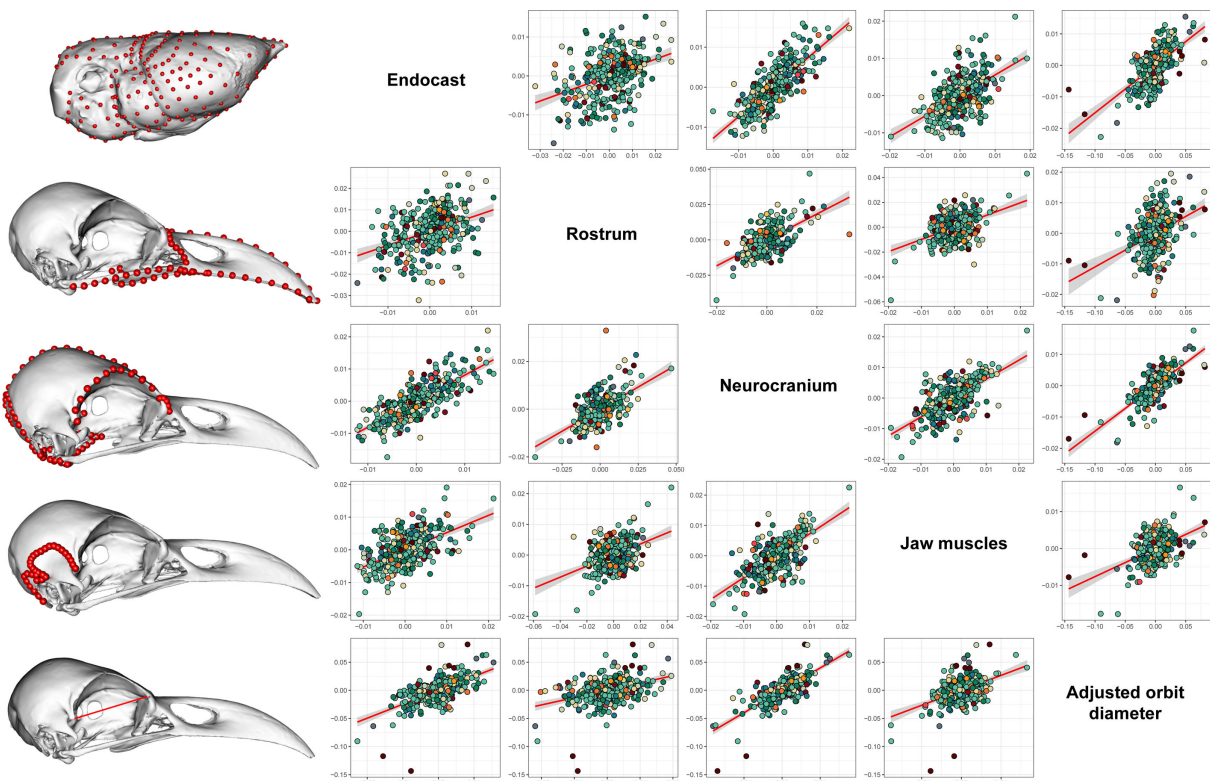


Figure 1. Results of two-block PLS analyses for all traits. Best fit lines are shown in red for each plot, with 95% confidence intervals represented by the shaded area, and points are coloured according to major clades, as per electronic supplementary material, figure S1. Each plot represents a pairwise comparison, with the axes specified by the intersection of traits read from the diagonal. For example, the top right plot is the two-block PLS of endocast shape (y-axis) and relative orbit diameter (x-axis). Plots are reflected across the diagonal, with x- and y-axes switched and representing a reversal of the regression formula for each pairwise comparison. Meshes in the leftmost column illustrate landmark positions for each trait on the endocast of *A. anhinga* (endocast, top row) and *Corvus albus* (skull, 2nd–5th rows).

Table 2. Phylogenetic half-lives with 95% parametric bootstrap (100 bootstrap replicates). Eigenvectors (columns) are arranged L–R in descending order of adaptive rate, represented by half-life as a percentage of total tree height (bottom row). Abbreviations in other rows correspond to traits: jaw muscle shape (MS), relative orbit diameter (ES), endocast shape (BS1 and BS2), neurocranial shape (NC) and rostrum shape (RS).

	directions (eigenvectors)					
	e_1	e_2	e_3	e_4	e_5	e_6
MS	0.992166	−0.031967	0.012604	−0.057689	0.129338	−0.001204
ES	0.060750	0.998903	0.014261	−0.057074	0.088845	−0.000785
BS1	−0.011620	−0.006464	0.929763	0.162063	−0.038512	0.000318
BS2	0.037994	0.017854	−0.366848	0.974235	0.176180	−0.001385
NC	0.101540	−0.028415	0.024467	−0.133959	0.962738	−0.014722
RS	0.005179	0.001576	−0.001496	0.008503	−0.126460	0.999890
half-life	62.46%	63.72%	65.11%	65.63%	73.52%	82.81%

4. Discussion

Our findings reveal that the avian head is shaped by the coordinated coevolution of skeletal and soft tissues, and that the interaction of these traits plays a major role in both generating and constraining phenotypic diversity in crown birds. In addition to known correlations between brain and neurocranial shape [38,48] and between brain shape and orbit size [26], our analyses reveal significant pairwise correlations between all examined traits (brain shape, RS, neurocranial shape, jaw MS and orbit diameter), and suggest that, although significant, allometry has a weak effect on trait integration. A common pattern seen in the two-block PLS analyses is that each trait yields similar trends of shape variation in response to shape variation in other traits, trends which are seen in the major axes of shape variation (electronic supplementary material, figures S4–S8). For example, RS varies along a continuum from short and curved to elongate and straight in all pairwise analyses (electronic supplementary material, figure S9). Similarly, the degree of ventral flexion of the endocast is associated with specific morphologies in all other traits (electronic supplementary material, figure S9). These results suggest that patterns of covariation of cranial traits are broadly consistent in birds and imply that shape constraints between traits play an important role in avian cranial evolution.

Significant correlation and coevolution among cranial traits can be explained by the shared signalling pathways which influence both brain and skull development in vertebrates, including FGF, TGF β , Wnt, Hedgehog and Notch [31,41,100].

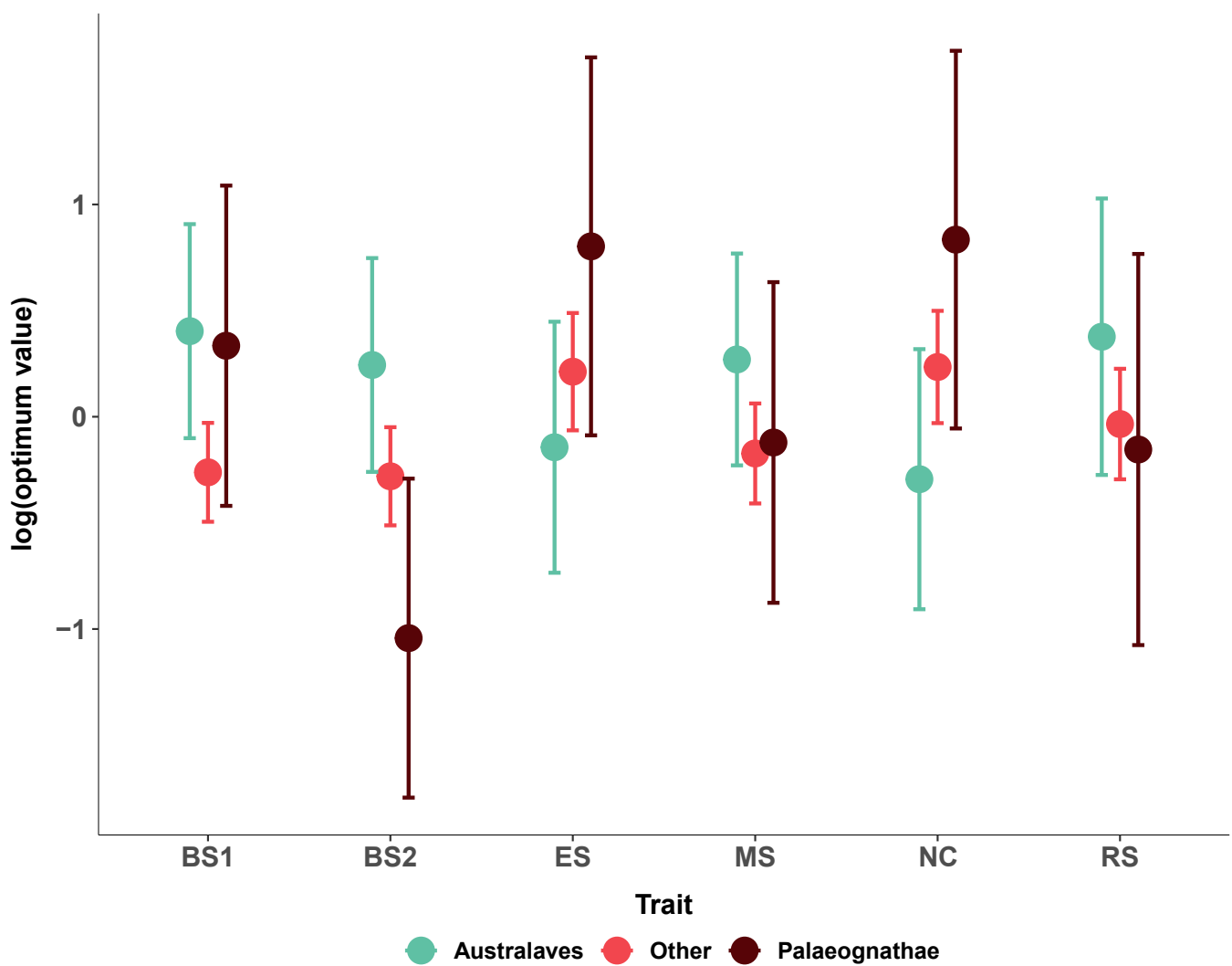


Figure 2. Deterministic optimum values of all traits for three subsets of species. Values are grouped according to trait (*x*-axis) and coloured according to group (see text for information).

This is reflected in the best-supported model in the *mvSLOUCH* analysis, Hand in Glove 2, which describes an adaptive evolutionary process where traits interact reciprocally via the neurocranium (table 1; electronic supplementary material, table S6). Traits do not all interact directly, however, and reciprocal interactions between traits imply that evolution of the head is not driven overwhelmingly by selection on one trait. Indeed, models which involve one-way, causal interactions between traits are generally poorly supported in our analyses. This is further supported by the relatively narrow range of half-lives across selection eigenvectors (table 2), which indicates that all have similar adaptation rates. Moreover, support for diagonal Σ_{yy} in this model indicates that there are no interactions between traits in the noise component of evolution, interactions typically associated with developmental constraints (e.g. allometry) or covariation with other, unmeasured traits [63,64].

Integration may allow rapid and extreme evolution along lines of least resistance in some radiations [57,61]. For example, the elongation trend observed in the main axis of variation of the whole skull, rostrum and neurocranium data (electronic supplementary material, figures S4–S6) is a common pattern of skull variation in many vertebrate groups and can be linked to integration because it tends to affect the entire skull [59–61,100–104]. Conversely, relaxed integration between elements can promote mosaic evolution by allowing them to respond to selection with some independence and may be linked to development [59,105]. For example, the rostrum and neurosensory regions of the avian head are largely derived from different developmental tissues, the mandibular cranial neural crest (rostrum) and mesoderm (brain/neurocranium). In the Hand in Glove model, the brain and rostrum do not interact directly, despite significant correlation, suggesting some degree of independent evolution. Further evidence that relaxed integration may play a role in cranial evolution, at least in some taxa, is provided by limited support in the *mvSLOUCH* analysis for the Modular model (AIC weight = 0.15), in which the neurosensory and rostrum form distinct non-interacting phenotypic modules. We recover the same patterns of trait coevolution after accounting for allometry, suggesting that the observed trait interactions and integration are not simply the result of allometric effects (electronic supplementary material, table S7).

Changes in the developmental timing and structural arrangement of the head have been linked to the early evolution of crown birds and the evolution of the avian beak and palate within Archosauria [31,35,55,106,107]. In more closely related taxa, studies of Darwin's finches (Fringillidae, Passeriformes) have shown that beak elongation in some taxa is due to higher levels of calmodulin (CaM) expression in the developing rostrum [30]. Similarly, misexpression of Bmp4 in the mesenchyme

of the upper rostrum in embryonic domestic chickens results in the development of deep rostral morphology resembling that of the Galapagos finch *Geospiza magnirostris* [29]. The ability of regions of the head to develop and evolve with a degree of independence is a hallmark of modularity [108] and has allowed rostrum shape to dominate morphological variation in adult birds (electronic supplementary material, figure S4) [56,60,62]. Beak shape has been linked to foraging ecology, suggesting it is under strong adaptive selection [58,109,110]. Moreover, the evolution of powered kinesis in the neognath skull has been suggested as a key evolutionary innovation, increasing the mechanical efficiency of jaw muscles and improving craniofacial dexterity in the absence of dextrous forelimbs [28]. The ability of the rostrum to explore novel morphologies and adapt its mechanical properties to a range of food sources without directly impacting brain shape may be a product of reduced integration between it and the brain, which may be responding to different adaptive pressures or functional needs.

Our findings do not contradict either of the other developmental hypotheses outlined in the introduction (Spatial Packing and Functional Matrix), and there is experimental evidence that each plays a role in shaping the vertebrate head during embryogenesis and development [41,48,53,111]. Notably, the key role of the brain in morphogenesis of the vertebrate head is known from many developmental studies [33–35,37,41,112,113]. Our findings confirm that the brain is evolutionarily integrated with the skull and that reciprocal interactions between different regions combine to influence head morphology across crown birds. Correlation between traits suggests that important constraints exist between regions of the avian head (figure 1) and lends some support to the SPH, though we cannot definitively state whether these correlations constitute trade-offs based on shape data alone because of the difficulty of determining if a change in shape of one trait has a detrimental effect on the shape of another [27]. While the OU models that we label SPH (table 1, Models 3–5) each involve brain shape directly influencing the evolution of other traits [48], the best-supported model in our analysis (table 1, Model 2) could also be interpreted as a form of spatial packing because of the reciprocal interactions among traits. Constraints between all traits may not be universal, however, and evidence for correlation between brain shape and jaw muscle morphology is more mixed. On the one hand, the two-block PLS result indicates that there is a correlation between these two traits. Conversely, OU models that include causal interactions between brain shape and jaw MS have a much lower likelihood than those without (electronic supplementary material, table S6).

Incorporating reciprocal interactions into models generally results in better support (electronic supplementary material, table S6), suggesting that peripheral soft tissues may moderate phenotypic evolution of the neurocranium and may provide some support to the Functional Matrix Hypothesis. Nonetheless, our interpretation of this hypothesis, where variation in brain shape, orbit size, jaw MS and RS influence the shape of the neurocranium, is not well-supported (electronic supplementary material, table S6). Although the Functional Matrix Hypothesis plays an established role in development [53], its effects on evolutionary morphology may be masked by larger-scale trends in shape evolution.

We have shown that interactions among traits in the avian head play an important role in regulating phenotypic evolution across crown birds. The brain is known to be a key influence on the development of surrounding cranial tissues, but our results emphasize the role that other cranial elements play in moderating morphological evolution of the avian head. Nonetheless, the patterns of trait covariation across crown birds are complex and are clearly the result of interactions of the multivariate shape space. Current methods of multivariate analysis only allow for a relatively small number of these dimensions to be analysed simultaneously and restrict us to major axes of shape variation, but improvements in methodology will allow for more nuanced analyses incorporating greater detail in both shape variation and taxon sampling. Our sample is composed exclusively of extant and recently extinct contemporary crown birds, and we cannot determine if the patterns of trait coevolution that we have found extend to more basal taxa that may not display the traits we associate with modern birds [3]. Incorporating basal taxa may thus reveal different patterns of trait evolution earlier in the evolutionary history of birds. Nonetheless, our sample is representative of the phenotypic diversity of modern birds and reveals a great deal about their >100 Ma evolutionary history [114]. The coordinated coevolution of cranial traits and the pattern by which they influence one another across crown birds highlights the importance of assessing the adaptive evolution of phenotypic traits in their developmental and evolutionary context and ultimately has implications for broad-scale studies of phenotypic evolution and trait integration.

Ethics. This work did not require ethical approval from a human subject or animal welfare committee.

Data accessibility. All data and code used in this study can be accessed on Dryad [115]. Supplementary material is available online [116].

Declaration of AI use. We have not used AI-assisted technologies in creating this article.

Authors' contributions. A.K.: conceptualization, data curation, formal analysis, investigation, methodology, software, writing—original draft; T.W.: conceptualization, data curation, investigation, resources, writing—original draft; C.E.: conceptualization, methodology, writing—original draft; R.N.F.: conceptualization, data curation, formal analysis, investigation, methodology, supervision, writing—original draft.

All authors gave final approval for publication and agreed to be held accountable for the work performed therein.

Conflict of interests. We declare we have no competing interests.

Funding. This work was funded by UK Research and Innovation (UKRI) under the UK government's Horizon Europe funding guarantee EP/Y010256/1 – BRAIN-DRAIN to R.N.F.

Acknowledgements. We thank Brett Clark, Mike Day and Agnese Lanzetti (NHMUK) for their help with specimen access and scanning, and other collections staff and researchers who made scan data available on MorphoSource. Ryan Marek (UCL) and Katherine Steinfield (University of Konstanz) provided additional scans, and R.M. provided the code used to construct our phylogeny. Laura Porro (UCL) found and collected the woodcock (*Scolopax rusticola*) used in this study. We thank Guillermo Navalón, two anonymous reviewers and the associate editor for thoughtful and instructive comments that helped improve our manuscript.

References

- Balanoff AM, Bever GS, Rowe TB, Norell MA. 2013 Evolutionary origins of the avian brain. *Nature* **501**, 93–96. (doi:10.1038/nature12424)

2. Early CM, Ridgely RC, Witmer LM. 2020 Beyond endocasts: using predicted brain-structure volumes of extinct birds to assess neuroanatomical and behavioral inferences. *Diversity &amp;lt;/i> **12**, 34. (doi:[10.3390/d12010034](https://doi.org/10.3390/d12010034))*
3. Field DJ, Burton MG, Benito J, Plateau O, Navalón G. 2025 Whence the birds: 200 years of dinosaurs, avian antecedents. *Biol. Lett.* **21**, 20240500. (doi:[10.1098/rsbl.2024.0500](https://doi.org/10.1098/rsbl.2024.0500))
4. Marugán-Lobón J, Watanabe A, Kawabe S. 2016 Studying avian encephalization with geometric morphometrics. *J. Anat.* **229**, 191–203. (doi:[10.1111/joa.12476](https://doi.org/10.1111/joa.12476))
5. Torres CR, Norell MA, Clarke JA. 2021 Bird neurocranial and body mass evolution across the end-Cretaceous mass extinction: the avian brain shape left other dinosaurs behind. *Sci. Adv.* **7**, eabg7099. (doi:[10.1126/sciadv.abg7099](https://doi.org/10.1126/sciadv.abg7099))
6. Tsuboi M *et al.* 2018 Breakdown of brain–body allometry and the encephalization of birds and mammals. *Nat. Ecol. Evol.* **2**, 1492–1500. (doi:[10.1038/s41559-018-0632-1](https://doi.org/10.1038/s41559-018-0632-1))
7. Wylie DR, Gutiérrez-Ibáñez C, Iwaniuk AN. 2015 Integrating brain, behavior, and phylogeny to understand the evolution of sensory systems in birds. *Front. Neurosci.* **9**, 281. (doi:[10.3389/fnins.2015.00281](https://doi.org/10.3389/fnins.2015.00281))
8. Corfield JR, Wild JM, Parsons S, Kubke MF. 2012 Morphometric analysis of telencephalic structure in a variety of neognath and paleognath bird species reveals regional differences associated with specific behavioral traits. *Brain Behav. Evol.* **80**, 181–195. (doi:[10.1159/000339828](https://doi.org/10.1159/000339828))
9. Güntürkün O, Pusch R, Rose J. 2024 Why birds are smart. *Trends Cogn. Sci.* **28**, 2023. (doi:[10.1016/j.tics.2023.11.002](https://doi.org/10.1016/j.tics.2023.11.002))
10. Heldstab SA, Isler K, Gruber SM, Schuppli C, van Schaik CP. 2022 The economics of brain size evolution in vertebrates. *Curr. Biol.* **32**, R697–R708. (doi:[10.1016/j.cub.2022.04.096](https://doi.org/10.1016/j.cub.2022.04.096))
11. Jerison HJ. 1985 Animal intelligence as encephalization. *Phil. Trans. R. Soc. Lond. B* **308**, 21–35. (doi:[10.1098/rstb.1985.0007](https://doi.org/10.1098/rstb.1985.0007))
12. Olkowicz S, Kocourek M, Lučan RK, Porteš M, Fitch WT, Herculano-Houzel S, Němec P. 2016 Birds have primate-like numbers of neurons in the forebrain. *Proc. Natl Acad. Sci. USA* **113**, 7255–7260. (doi:[10.1073/pnas.1517131113](https://doi.org/10.1073/pnas.1517131113))
13. Balanoff AM, Smaers JB, Turner AH. 2016 Brain modularity across the theropod–bird transition: testing the influence of flight on neuroanatomical variation. *J. Anat.* **229**, 204–214. (doi:[10.1111/joa.12403](https://doi.org/10.1111/joa.12403))
14. Iwaniuk AN, Hurd PL. 2005 The evolution of cerebrotypes in birds. *Brain Behav. Evol.* **65**, 215–230. (doi:[10.1159/000084313](https://doi.org/10.1159/000084313))
15. Vincze O, Vágási CI, Pap PL, Osváth G, Möller AP. 2015 Brain regions associated with visual cues are important for bird migration. *Biol. Lett.* **11**, 20150678. (doi:[10.1098/rsbl.2015.0678](https://doi.org/10.1098/rsbl.2015.0678))
16. Ksepka DT *et al.* 2020 Tempo and pattern of avian brain size evolution. *Curr. Biol.* **30**, 2026–2036. (doi:[10.1016/j.cub.2020.03.060](https://doi.org/10.1016/j.cub.2020.03.060))
17. Watanabe A, Balanoff AM, Gignac PM, Gold MEL, Norell MA. 2021 Novel neuroanatomical integration and scaling define avian brain shape evolution and development. *eLife* **10**, e68809. (doi:[10.7554/elife.68809](https://doi.org/10.7554/elife.68809))
18. Jerison HJ. 1973 *Evolution of the brain and intelligence*. New York, NY: Academic Press.
19. Ashwell KWS, Scofield RP. 2008 Big birds and their brains: paleoneurology of the New Zealand Moa. *Brain Behav. Evol.* **71**, 151–166. (doi:[10.1159/000111461](https://doi.org/10.1159/000111461))
20. Early CM, Iwaniuk AN, Ridgely RC, Witmer LM. 2020 Endocast structures are reliable proxies for the sizes of corresponding regions of the brain in extant birds. *J. Anat.* **237**, 1162–1176. (doi:[10.1111/joa.13285](https://doi.org/10.1111/joa.13285))
21. Gold MEL, Bourdon E, Norell MA. 2016 The first endocast of the extinct dodo (*Raphus cucullatus*) and an anatomical comparison amongst close relatives (Aves, Columbiformes). *Zool. J. Linn. Soc.* **177**, 950–963. (doi:[10.1111/zoj.12388](https://doi.org/10.1111/zoj.12388))
22. Iwaniuk AN, Nelson JE. 2002 Can endocranial volume be used as an estimate of brain size in birds? *Can. J. Zool.* **80**, 16–23. (doi:[10.1139/z01-204](https://doi.org/10.1139/z01-204))
23. Roth G, Dicke U. 2005 Evolution of the brain and intelligence. *Trends Cogn. Sci.* **9**, 250–257. (doi:[10.1016/j.tics.2005.03.005](https://doi.org/10.1016/j.tics.2005.03.005))
24. Emery NJ. 2006 Cognitive ornithology: the evolution of avian intelligence. *Phil. Trans. R. Soc. Lond. B* **361**, 23–43. (doi:[10.1098/rstb.2005.1736](https://doi.org/10.1098/rstb.2005.1736))
25. Isler K, van Schaik C. 2006 Costs of encephalization: the energy trade-off hypothesis tested on birds. *J. Hum. Evol.* **51**, 228–243. (doi:[10.1016/j.jhevol.2006.03.006](https://doi.org/10.1016/j.jhevol.2006.03.006))
26. Kawabe S, Shimokawa T, Miki H, Matsuda S, Endo H. 2013 Variation in avian brain shape: relationship with size and orbital shape. *J. Anat.* **223**, 495–508. (doi:[10.1111/joa.12109](https://doi.org/10.1111/joa.12109))
27. Garland T, Downs CJ, Ives AR. 2022 Trade-offs (and constraints) in organismal biology. *Physiol. Biochem. Zool.* **95**, 82–112. (doi:[10.1086/717897](https://doi.org/10.1086/717897))
28. Wilken AT, Sellers KC, Cost IN, Davis J, Middleton KM, Witmer LM, Holliday CM. 2025 Avian cranial kinesis is the result of increased encephalization during the origin of birds. *Proc. Natl Acad. Sci. USA* **122**, e2411138122. (doi:[10.1073/pnas.2411138122](https://doi.org/10.1073/pnas.2411138122))
29. Abzhanov A, Protas M, Grant BR, Grant PR, Tabin CJ. 2004 *Bmp4* and morphological variation of beaks in Darwin's finches. *Science* **305**, 1462–1465. (doi:[10.1126/science.1098095](https://doi.org/10.1126/science.1098095))
30. Abzhanov A, Kuo WP, Hartmann C, Grant BR, Grant PR, Tabin CJ. 2006 The calmodulin pathway and evolution of elongated beak morphology in Darwin's finches. *Nature* **442**, 563–567. (doi:[10.1038/nature04843](https://doi.org/10.1038/nature04843))
31. Bhullar BAS, Morris ZS, Sefton EM, Tok A, Tokita M, Namkoong B, Camacho J, Burnham DA, Abzhanov A. 2015 A molecular mechanism for the origin of a key evolutionary innovation, the bird beak and palate, revealed by an integrative approach to major transitions in vertebrate history. *Evolution* **69**, 1665–1677. (doi:[10.1111/evo.12684](https://doi.org/10.1111/evo.12684))
32. Conith AJ, Hope SA, Albertson RC. 2023 Covariation of brain and skull shapes as a model to understand the role of crosstalk in development and evolution. *Evol. Dev.* **25**, 85–102. (doi:[10.1111/ede.12421](https://doi.org/10.1111/ede.12421))
33. Hu D, Marcucio RS. 2009 A SHH-responsive signaling center in the forebrain regulates craniofacial morphogenesis via the facial ectoderm. *Development* **136**, 107–116. (doi:[10.1242/dev.026583](https://doi.org/10.1242/dev.026583))
34. Hu D, Young NM, Xu Q, Jamniczky H, Green RM, Mio W, Marcucio RS, Hallgrímsson B. 2015 Signals from the brain induce variation in avian facial shape. *Dev. Dyn.* **244**, 1133–1143. (doi:[10.1002/dvdy.24284](https://doi.org/10.1002/dvdy.24284))
35. Hüppi E, Werneburg I, Sánchez-Villagra MR. 2021 Evolution and development of the bird chondrocranium. *Front. Zool.* **18**, 21. (doi:[10.1186/s12983-021-00406-z](https://doi.org/10.1186/s12983-021-00406-z))
36. Francis-West PH, Robson L, Evans DJR. 2003 Craniofacial development the tissue and molecular interactions that control development of the head. In *Advances in anatomy and cell biology* (eds F Beck, B Christ), p. III–VI, vol. **169**. Berlin, Heidelberg, Germany: Springer-Verlag. (doi:[10.1007/978-3-642-55570-1](https://doi.org/10.1007/978-3-642-55570-1))
37. Marcucio RS, Cordero DR, Hu D, Helms JA. 2005 Molecular interactions coordinating the development of the forebrain and face. *Dev. Biol.* **284**, 48–61. (doi:[10.1016/j.ydbio.2005.04.030](https://doi.org/10.1016/j.ydbio.2005.04.030))
38. Fabbri M *et al.* 2017 The skull roof tracks the brain during the evolution and development of reptiles including birds. *Nat. Ecol. Evol.* **1**, 1543–1550. (doi:[10.1038/s41559-017-0288-2](https://doi.org/10.1038/s41559-017-0288-2))
39. Watanabe A, Gignac PM, Balanoff AM, Green TL, Kley NJ, Norell MA. 2018 Are endocasts good proxies for brain size and shape in archosaurs throughout ontogeny? *J. Anat.* **234**, 291–305. (doi:[10.1111/joa.12918](https://doi.org/10.1111/joa.12918))
40. Holliday CM. 2009 New insights into dinosaur jaw muscle anatomy. *Anat. Rec.* **292**, 1246–1265. (doi:[10.1002/ar.20982](https://doi.org/10.1002/ar.20982))
41. Richtsmeier JT, Flaherty K. 2013 Hand in glove: brain and skull in development and dysmorphogenesis. *Acta Neuropathol.* **125**, 469–489. (doi:[10.1007/s00401-013-1104-y](https://doi.org/10.1007/s00401-013-1104-y))
42. Richtsmeier JT, Aldridge K, Eleon VBD, Panchal J, Kane AA, Marsh JL, Yan P, Cole TM. 2006 Phenotypic integration of neurocranium and brain. *J. Exp. Zool.* **306**, 360–378. (doi:[10.1002/jez.b.21092](https://doi.org/10.1002/jez.b.21092))
43. Jeffery NS, Sarver DC, Mendias CL. 2021 Ontogenetic and *in silico* models of spatial-packing in the hypermuscular mouse skull. *J. Anat.* **238**, 1284–1295. (doi:[10.1111/joa.13393](https://doi.org/10.1111/joa.13393))

44. Jeffery N, Mendias C. 2014 Endocranial and masticatory muscle volumes in myostatin-deficient mice. *R. Soc. Open Sci.* **1**, 140187. (doi:10.1098/rsos.140187)
45. Cerio DG, Llera Martín CJ, Hogan AVC, Balanoff AM, Watanabe A, Bever GS. 2023 Differential growth of the adductor muscles, eyeball, and brain in the chick *Gallus gallus* with comments on the fossil record of stem-group birds. *J. Morphol.* **284**, e21622. (doi:10.1002/jmor.21622)
46. Burton RF. 2008 The scaling of eye size in adult birds: relationship to brain, head and body sizes. *Vis. Res.* **48**, 2345–2351. (doi:10.1016/j.visres.2008.08.001)
47. Lieberman DE, Hallgrímsson B, Liu W, Parsons TE, Jamniczky HA. 2008 Spatial packing, cranial base angulation, and craniofacial shape variation in the mammalian skull: testing a new model using mice. *J. Anat.* **212**, 720–735. (doi:10.1111/j.1469-7580.2008.00900.x)
48. Marugán-Lobón J, Nebreda SM, Navalón G, Benson RBJ. 2022 Beyond the beak: brain size and allometry in avian craniofacial evolution. *J. Anat.* **240**, 197–209. (doi:10.1111/joa.13555)
49. Ross CF, Ravosa MJ. 1993 Basicranial flexion, relative brain size, and facial kyphosis in nonhuman primates. *Am. J. Phys. Anthropol.* **91**, 305–324. (doi:10.1002/ajpa.1330910306)
50. Moss ML, Young RW. 1960 A functional approach to craniology. *Am. J. Phys. Anthropol.* **18**, 281–292. (doi:10.1002/ajpa.1330180406)
51. Moss ML. 1971 Neurotrophic processes in orofacial growth. *J. Dent. Res.* **50**, 1492–1494. (doi:10.1177/00220345710500062301)
52. Moss ML. 1997 The functional matrix hypothesis revisited. 1. The role of mechanotransduction. *Am. J. Orthod. Dentofac. Orthop.* **112**, 8–11. (doi:10.1016/s0889-5406(97)70267-1)
53. Kyrganides S, Moore T, Miller JH, Tallents RH. 2011 Melvin Moss' function matrix theory—revisited. *Orthod. Waves* **70**, odw.2010.07.001. (doi:10.1016/j.odw.2010.07.001)
54. Klingenberg CP, Marugán-Lobón J. 2013 Evolutionary covariation in geometric morphometric data: analyzing integration, modularity, and allometry in a phylogenetic context. *Syst. Biol.* **62**, 591–610. (doi:10.1093/sysbio/syt025)
55. Bhullar BAS, Hanson M, Fabbri M, Pritchard A, Bever GS, Hoffman E. 2016 How to make a bird skull: major transitions in the evolution of the avian cranium, Paedomorphosis, and the beak as a surrogate hand. *Integr. Comp. Biol.* **56**, 389–403. (doi:10.1093/icb/icw069)
56. Bright JA, Marugán-Lobón J, Cobb SN, Rayfield EJ. 2016 The shapes of bird beaks are highly controlled by nondietary factors. *Proc. Natl. Acad. Sci.* **113**, 5352–5357. (doi:10.1073/pnas.1602683113)
57. Cooney CR, Bright JA, Capp EJR, Chira AM, Hughes EC, Moody CJA, Nouri LO, Varley ZK, Thomas GH. 2017 Mega-evolutionary dynamics of the adaptive radiation of birds. *Nature* **542**, 344–347. (doi:10.1038/nature21074)
58. Bright JA, Marugán-Lobón J, Rayfield EJ, Cobb SN. 2019 The multifactorial nature of beak and skull shape evolution in parrots and cockatoos (Psittaciformes). *BMC Evol. Biol.* **19**, 1–9. (doi:10.1186/s12862-019-1432-1)
59. Felice RN, Goswami A. 2018 Developmental origins of mosaic evolution in the avian cranium. *Proc. Natl. Acad. Sci. USA* **115**, 555–560. (doi:10.1073/pnas.1716437115)
60. Felice RN, Tobias JA, Pigot AL, Goswami A. 2019 Dietary niche and the evolution of cranial morphology in birds. *Proc. R. Soc. B* **286**, 20182677. (doi:10.1098/rspb.2018.2677)
61. Navalón G, Marugán-Lobón J, Bright JA, Cooney CR, Rayfield EJ. 2020 The consequences of craniofacial integration for the adaptive radiations of Darwin's finches and Hawaiian honeycreepers. *Nat. Ecol. Evol.* **4**, 270–278. (doi:10.1038/s41559-019-1092-y)
62. Stefanini MI, Milla Carmona PS, Gómez-Bahamón V, Mongiardino Koch N, Soto IM, Gómez RO, Zyskowski K, Tambussi CP. 2025 Craniofacial modularity and the evolution of cranial kinesis in the adaptive radiation of Furnariidae (Aves: Passeriformes). *Evolution* **79**, 625–640. (doi:10.1093/evolut/qpaf013)
63. Bartoszek K, Pienaar J, Mostad P, Andersson S, Hansen TF. 2012 A phylogenetic comparative method for studying multivariate adaptation. *J. Theor. Biol.* **314**, 204–215. (doi:10.1016/j.jtbi.2012.08.005)
64. Bartoszek K, Tredgett Clarke J, Fuentes-González J, Mitov V, Pienaar J, Piwczyński M, Puchałka R, Spalik K, Voje KL. 2024 Fast mvSLOUCH: Multivariate Ornstein–Uhlenbeck-based models of trait evolution on large phylogenies. *Methods Ecol. Evol.* **15**, 1507–1515. (doi:10.1111/2041-210x.14376)
65. Gill F, Donsker D, Rasmussen P (eds). 2024 IOC world bird list (v15.1).
66. Dragonfly 2022.2. 2022 Dragonfly 2022.2 (Computer software). Montreal, Canada: Comet Technologies Canada Inc. See <https://www.theobjects.com/dragonfly>.
67. VGStudio Max 3.5.x. 2023 VGStudio Max 3.5.x (computer software). Heidelberg, Germany: Volume Graphics GmbH. See <https://www.volumegraphics.com/en/products/vgsm.html>.
68. Profico A, Buzi C, Castiglione S. 2023 Arothron: geometric morphometric methods and virtual anthropology tools. (doi:10.1002%2Fajpa.24340)
69. Stiller J *et al.* 2024 Complexity of avian evolution revealed by family-level genomes. *Nature* **629**, 851–860. (doi:10.1038/s41586-024-07323-1)
70. Jetz W, Thomas GH, Joy JB, Hartmann K, Mooers AO. 2012 The global diversity of birds in space and time. *Nature* **491**, 444–448. (doi:10.1038/nature11631)
71. Drummond AJ, Rambaut A. 2007 BEAST: Bayesian evolutionary analysis by sampling trees. *BMC Evol. Biol.* **7**, 214. (doi:10.1186/1471-2148-7-214)
72. Cooney CR, Thomas GH. 2021 Heterogeneous relationships between rates of speciation and body size evolution across vertebrate clades. *Nat. Ecol. Evol.* **5**, 101–110. (doi:10.1038/s41559-020-01321-y)
73. Oliveros CH *et al.* 2019 Earth history and the passerine superradiation. *Proc. Natl. Acad. Sci. USA* **116**, 7916–7925. (doi:10.1073/pnas.1813206116)
74. Castiglione S, Tesone G, Piccolo M, Melchionna M, Mondanaro A, Serio C, Di Febbraro M, Raia P. 2018 A new method for testing evolutionary rate variation and shifts in phenotypic evolution. *Methods Ecol. Evol.* **9**, 974–983. (doi:10.1111/2041-210x.12954)
75. Cole TL *et al.* 2019 Mitogenomes uncover extinct penguin taxa and reveal island formation as a key driver of speciation. *Mol. Biol. Evol.* **36**, 784–797. (doi:10.1093/molbev/msz017)
76. Dumbacher J. 2003 Phylogeny of the owllet-nightjars (Aves: Aegothelidae) based on mitochondrial DNA sequence. *Mol. Phylogenetics Evol.* **29**, 540–549. (doi:10.1016/s1055-7903(03)00135-0)
77. Garcia-R JC, Gibb GC, Trewick SA. 2014 Deep global evolutionary radiation in birds: diversification and trait evolution in the cosmopolitan bird family Rallidae. *Mol. Phylogenetics Evol.* **81**, 96–108. (doi:10.1016/j.ympev.2014.09.008)
78. Musser GM, Cracraft J. 2019 A new morphological dataset reveals a novel relationship for the Adzebills of New Zealand (*Aptornis*) and provides a foundation for total evidence neoavian phylogenetics. *Am. Mus. Novit.* **2019**, 170. (doi:10.1206/3927.1)
79. Shapiro B, Sibthorpe D, Rambaut A, Austin J, Wragg GM, Bininda-Emonds ORP, Lee PLM, Cooper A. 2002 Flight of the Dodo. *Science* **295**, 1683–1683. (doi:10.1126/science.295.5560.1683)
80. Yonezawa T *et al.* 2017 Phylogenomics and morphology of extinct paleognaths reveal the origin and evolution of the ratites. *Curr. Biol.* **27**, 68–77. (doi:10.1016/j.cub.2016.10.029)
81. Mitchell MJ, Goswami A, Felice RN. 2021 Cranial integration in the ring-necked parakeet, *Psittacula krameri* (Psittaciformes: Psittaculidae). *Biol. J. Linn. Soc.* **133**, 47–56. (doi:10.1093/biolinnean/blab032)
82. Stratovan Checkpoint v. 2020.10.13.0859. 2020 Stratovan Corporation. See <https://www.stratovan.com/products/checkpoint>.
83. Baumel JJ, King AS, Breazile JE, Evans HE, Vanden Berge JC. 1993 *Handbook of avian anatomy: Nomina Anatomica Avium*, pp. 228–230, 2nd edn. Cambridge, MA: Publications of the Nuttall Ornithological Club.
84. Livezey L, Zusi Z, Litwak T. 2006 Higher-order phylogeny of modern birds (*Theropoda*, Aves: Neornithes) based on comparative anatomy. In *Polish archives of internal medicine*, vol. 1. Carnegie Museum of Natural History. (doi:10.2992/0145-9058(2006)37[1:PON]2.0.CO;2)

85. Watanabe A. 2018 How many landmarks are enough to characterize shape and size variation? *PLoS One* **13**, e0198341. (doi:[10.1371/journal.pone.0198341](https://doi.org/10.1371/journal.pone.0198341))
86. Schlager S. 2017 Morpho and Rvcg – shape analysis in R. In *Statistical shape and deformation analysis* (eds G Zheng, S Li, G Szekely), pp. 217–256. London, UK: Academic Press. (doi:[10.1016/B978-0-12-810493-4.00011-0](https://doi.org/10.1016/B978-0-12-810493-4.00011-0))
87. Bardua C, Felice RN, Watanabe A, Fabre AC, Goswami A. 2019 A practical guide to sliding and surface semilandmarks in morphometric analyses. *Integr. Org. Biol.* **1**, z016. (doi:[10.1093/iob/obz016](https://doi.org/10.1093/iob/obz016))
88. Ollonen J *et al.* 2024 Dynamic evolutionary interplay between ontogenetic skull patterning and whole-head integration. *Nat. Ecol. Evol.* **8**, 536–551. (doi:[10.1038/s41559-023-02295-3](https://doi.org/10.1038/s41559-023-02295-3))
89. Zelditch ML, Swiderski DL, Sheets HD, Fink WL. 2004 *Geometric morphometrics for biologists: a primer*. London, UK: Elsevier Inc.
90. Adams DC, Collyer ML, Kaliontzopoulou A, Baken E. 2023 Geomorph: software for geometric morphometric analyses. R package version 4.0.6. See <https://cran.r-project.org/package=geomorph>.
91. Klingenberg CP. 2016 Size, shape, and form: concepts of allometry in geometric morphometrics. *Dev. Genes Evol.* **226**, 113–137. (doi:[10.1007/s00427-016-0539-2](https://doi.org/10.1007/s00427-016-0539-2))
92. Hallgrímsson B, Katz DC, Aponte JD, Larson JR, Devine J, Gonzalez PN, Young NM, Roseman CC, Marcucio RS. 2019 Integration and the developmental genetics of Allometry. *Integr. Comp. Biol.* **59**, 1369–1381. (doi:[10.1093/icb/icz105](https://doi.org/10.1093/icb/icz105))
93. Tobias JA *et al.* 2022 AVONET: morphological, ecological and geographical data for all birds. *Ecol. Lett.* **25**, 581–597. (doi:[10.1111/ele.13898](https://doi.org/10.1111/ele.13898))
94. Field DJ, Lynner C, Brown C, Darroch SAF. 2013 Skeletal correlates for body mass estimation in modern and fossil flying birds. *PLoS One* **8**, e82000. (doi:[10.1371/journal.pone.0082000](https://doi.org/10.1371/journal.pone.0082000))
95. Adams DC, Felice RN. 2014 Assessing phylogenetic morphological integration and trait covariation in morphometric data using evolutionary covariance matrices. *PLoS One* **9**, 94335. (doi:[10.1371/journal.pone.0094335](https://doi.org/10.1371/journal.pone.0094335))
96. Adams DC, Collyer ML. 2016 On the comparison of the strength of morphological integration across morphometric datasets. *Evolution* **70**, 2623–2631. (doi:[10.1111/evo.13045](https://doi.org/10.1111/evo.13045))
97. Baken EK, Collyer ML, Kaliontzopoulou A, Adams DC. 2021 geomorph v4.0 and gmShiny: enhanced analytics and a new graphical interface for a comprehensive morphometric experience. *Methods Ecol. Evol.* **12**, 2355–2363. (doi:[10.1111/2041-210x.13723](https://doi.org/10.1111/2041-210x.13723))
98. Cardini A. 2019 Integration and modularity in procrustes shape data: is there a risk of spurious results? *Evol. Biol.* **46**, 90–105. (doi:[10.1007/s11692-018-9463-x](https://doi.org/10.1007/s11692-018-9463-x))
99. Grabowski M *et al.* 2023 A cautionary note on ‘A cautionary note on the use of Ornstein Uhlenbeck models in macroevolutionary studies’. *Syst. Biol.* **72**, 955–963. (doi:[10.1093/sysbio/syad012](https://doi.org/10.1093/sysbio/syad012))
100. Fabre AC *et al.* 2020 Metamorphosis shapes cranial diversity and rate of evolution in salamanders. *Nat. Ecol. Evol.* **4**, 1129–1140. (doi:[10.1038/s41559-020-1225-3](https://doi.org/10.1038/s41559-020-1225-3))
101. Neben CL, Merrill AE. 2015 Chapter eighteen – signaling pathways in craniofacial development: insights from rare skeletal disorders. In *Current topics in developmental biology craniofacial development* (ed. Y Chai), pp. 493–542, vol. **115**. London, UK: Academic Press. (doi:[10.1016/bs.ctdb.2015.09.005](https://doi.org/10.1016/bs.ctdb.2015.09.005))
102. Goswami A *et al.* 2022 Attenuated evolution of mammals through the Cenozoic. *Science* **378**, 377–383. (doi:[10.1126/science.abm7525](https://doi.org/10.1126/science.abm7525))
103. Knapp A, Rangel-de Lázaro G, Friedman M, Johanson Z, Evans KM, Giles S, Beckett HT, Goswami A. 2023 How to tuna fish: constraint, convergence, and integration in the neurocranium of pelagician fishes. *Evolution* **77**, 1277–1288. (doi:[10.1093/evolut/qpad056](https://doi.org/10.1093/evolut/qpad056))
104. Watanabe A, Fabre AC, Felice RN, Maisano JA, Müller J, Herrel A, Goswami A. 2019 Ecomorphological diversification in squamates from conserved pattern of cranial integration. *PNAS* **116**, 14688–14697. (doi:[10.1073/pnas.1820967116](https://doi.org/10.1073/pnas.1820967116))
105. Maddin HC, Piekarski N, Sefton EM, Hanken J. 2016 Homology of the cranial vault in birds: new insights based on embryonic fate-mapping and character analysis. *R. Soc. Open Sci.* **3**, 160356. (doi:[10.1098/rsos.160356](https://doi.org/10.1098/rsos.160356))
106. Plateau O, Foth C. 2020 Birds have peramorphic skulls, too: anatomical network analyses reveal oppositional heterochronies in avian skull evolution. *Commun. Biol.* **3**, 195. (doi:[10.1038/s42003-020-0914-4](https://doi.org/10.1038/s42003-020-0914-4))
107. Yang TR, Sander PM. 2018 The origin of the bird’s beak: new insights from dinosaur incubation periods. *Biol. Lett.* **14**, 20180090. (doi:[10.1098/rsbl.2018.0090](https://doi.org/10.1098/rsbl.2018.0090))
108. Zelditch ML, Goswami A. 2021 What does modularity mean? *Evol. Dev.* **23**, 377–403. (doi:[10.1111/ede.12390](https://doi.org/10.1111/ede.12390))
109. Natale R, Slater GJ. 2022 The effects of foraging ecology and allometry on avian skull shape vary across levels of phylogeny. *Am. Nat.* **200**, E174–E188. (doi:[10.1086/720745](https://doi.org/10.1086/720745))
110. Navalón G, Bright JA, Marugán-Lobón J, Rayfield EJ. 2019 The evolutionary relationship among beak shape, mechanical advantage, and feeding ecology in modern birds. *Evolution* **73**, 422–435. (doi:[10.1111/evo.13655](https://doi.org/10.1111/evo.13655))
111. Marugán-Lobón J, Buscalioni ÁD. 2006 Avian skull morphological evolution: exploring exo- and endocranial covariation with two-block partial least squares. *Zoology* **109**, 217–230. (doi:[10.1016/j.zool.2006.03.005](https://doi.org/10.1016/j.zool.2006.03.005))
112. Le Douarin NM. 2004 The avian embryo as a model to study the development of the neural crest: a long and still ongoing story. *Mech. Dev.* **121**, 1089–1102. (doi:[10.1016/j.mod.2004.06.003](https://doi.org/10.1016/j.mod.2004.06.003))
113. Hanken J, Thorogood P. 1993 Evolution and development of the vertebrate skull: the role of pattern formation. *Trends Ecol. Evol.* **8**, 9–15. (doi:[10.1016/0169-5347\(93\)90124-8](https://doi.org/10.1016/0169-5347(93)90124-8))
114. Brocklehurst N, Field DJ. 2024 Tip dating and Bayes factors provide insight into the divergences of crown bird clades across the end-Cretaceous mass extinction. *Proc. R. Soc. B* **291**, 20232618. (doi:[10.1098/rspb.2023.2618](https://doi.org/10.1098/rspb.2023.2618))
115. Knapp A, West T, Early C, Felice R. 2025 Data for: Avian cranial evolution is influenced by shape interactions between hard and soft tissue traits. Dryad Digital Repository. (doi:[10.5061/dryad.sxksn03dp](https://doi.org/10.5061/dryad.sxksn03dp))
116. Knapp A, West T, Early C, Felice RN. 2025 Supplementary material from: Avian cranial evolution is influenced by shape interactions between hard and soft tissue traits. Figshare. (doi:[10.6084/m9.figshare.c.8168691](https://doi.org/10.6084/m9.figshare.c.8168691))